CROSS SECTIONS FOR THE CAPTURE OF SLOW ELECTRONS BY O_2 AND H_2O MOLECULES AND MOLECULES OF HALOGEN COMPOUNDS

I. S. BUCHEL'NIKOVA

Institute of Chemical Physics, Academy of Sciences, U.S.S.R.

Submitted to JETP editor, May 22, 1958; resubmitted July 21, 1958

J. Exptl. Theoret. Phys. (U.S.S.R.) 35, 1119-1130 (November, 1958)

Using a nearly-monoenergetic electron beam and the single-collision method, cross sections have been measured for the capture of slow electrons by the molecules SF_6, CCl_4, CF_3I, CCl_2F_2, BCl_3, HCl, and HBr; capture cross section for electrons with energies of several electron volts by O_2 and H_2O have also been measured. The width of the electron energy distribution was 0.2 to 0.3 ev; the energy was measured with an accuracy of 0.01 to 0.02 ev. The following values were found for the maximum cross sections: SF_6, 5.7×10^{-16} cm^2; CCl_4, 1.3×10^{-16} cm^2; CF_3I, 7.8×10^{-17} cm^2; CCl_2F_2, 5.4×10^{-17} cm^2; BCl_3, 2.8×10^{-17} cm^2; HBr, 5.8×10^{-17} cm^2; HCl, 3.9×10^{-18} cm^2; H_2O, 4.8×10^{-18} cm^2; O_2, 1.3×10^{-18} cm^2. It is found that the appearance potential for O^- in O_2 is 4.63 ± 0.04 ev; the appearance potential for H^- in H_2O is 5.45 ± 0.09 ev.

IN the present work we report on measurements of the cross sections for capture of slow electrons by SF_6, CCl_4, CF_3I, CCl_2F_2, BCl_3, HCl, HBr and the capture of electrons with energies of several electron volts by O_2 and H_2O. The measurements were carried out by the single-collision method, using a nearly-monoenergetic electron beam. The method of measurement is as follows.[1] A beam of electrons, which is collimated by a honeycomb diaphragm (divergence angle of 2°) and a magnetic field of 15 to 20 oersteds enters an equipotential region through a system of grids and then strikes a collector. Ions which are formed in the equipotential region are collected by a cylindrical electrode. To eliminate the effect of the cathode voltage drop on electron energy the cathode is heated by pulses and the electrons are extracted during the time in which heater current does not flow. In the path of the electron beam there is a diaphragm which is at a potential greater than the space-charge potential of the beam (1 to 1.5 volts). Only electrons with energies greater than this value pass through the diaphragm. The electron current is approximately $(1 \text{ to } 3) \times 10^{-8}$ amp, with a beam cross-sectional area of approximately 3 cm^2, so that space charge effects are negligibly small.

The energy distribution of the electron beam which passes through the diaphragm is exponential, with a sharp cut-off on the low-energy side; the width of the distribution is approximately 1 ev. By employing a nearly-monoenergetic beam[2] it is possible to reduce the width to 0.2 or 0.3 ev. The logarithm of the ion current for the monoenergetic component is found to be a linear function of the retarding potential; hence it may be assumed that the distribution in the monoenergetic component is exponential.

Provision is made for compensation of the contact potentials of the diaphragms and grids which define the equipotential region. The elements of the system are gold-plated in order to achieve stable contact potentials. By careful compensation of the contact potentials and avoidance of distortion of the electric fields in the equipotential region it is possible to determine the energy with an accuracy of the order of 0.02 ev.

The magnetic field makes it impossible for scattered electrons to reach the ion collector. Since the divergence angle of the electron beam is 2°, a beam of 15 to 20 oersteds is sufficient to eliminate scattering. Because of the small field the radii for ions with masses greater than 20 atomic mass units is greater than the radius of the ion collector; however, most of the ions strike the collector. By introducing corrections for the instrument geometry it is possible to determine the ion collection with an accuracy of the order of several percent.

Because the divergence angle of the beam is small, it is possible to determine the length of the electron path in the equipotential region with good accuracy. It should be noted that the solenoid which produces the magnetic field is posi-

tioned in such a way that increasing the field to 30 or 40 oersteds does not increase the number of electrons which pass through the diaphragm. Thus, there is no change in the effective divergence angle of the electron beam, or the path length, when the magnetic field is turned on.

The ion and electron currents are measured with electrometer amplifiers. The gas pressure is measured with an ionization gage which is calibrated against a McLeod gage for the gas being studied.

The measurements are carried out in the 0 to 1 ev and 0 to 3 ev electron-energy ranges. In the first case the ion and electron collectors are at zero potential with respect to the cathode and the current of scattered electrons is negligibly small. In the measurements in the energy region up to 3 ev, the collector potential is maintained at +4 volts and the scattered-electron current can be important. It is possible to estimate the current of scattered electrons from the current at the ion collector. In this case, the cross sections is calculated by subtracting the scattered-electron current from the current at the ion collector. It has been found that the cross-section values obtained in experiments without scattering and the values computed from the collector current (subtracting the scattered-electron component) are in agreement within the accuracy of the measurements. The capture cross section is computed from the formula

$$\sigma = \frac{I_i/\eta\xi}{(I_e/\beta)\cdot 3.55\cdot 10^{16}\cdot 273\,(\chi p/T)\,\lambda L},$$

where I_i is the ion current, I_e is the electron current, p is the gas pressure shown by the ionization gauge, χ is the conversion coefficient for converting the reading on the ionization gauge to the true pressure, T is the temperature of the operating region, L is the length of the operating region, β is a correction for interception of ions by the grids which shield the ion collector, ξ is a correction for ion loss, and λ is a correction introduced to average over paths of electrons which move at different angles. The total error in the corrections is approximately 20 to 25%.

In those cases in which the width of the capture region is smaller than or comparable with the width of the electron energy distribution the distribution is taken into account in computing the cross sections. Let I(V) be the observed dependence of ion current on accelerating potential and $N_e(U)\,dU$ the number of electrons with energies between U and U + dU; in the present case $N_e(U) = N_0 \exp\{-U/kT\}$ and E = U + V is the total electron energy. Then

$$I(V) = \int_0^\infty A\sigma(E)\,N_0 e^{-U/kT}dU,$$

where $A = 969.15 \times 10^{16}\,\eta\xi\chi p\lambda L/\beta t$. Converting to the variable E, we have

$$I(V) = AN_0 e^{V/kT}\int_V^\infty \sigma(E)\,e^{-E/kT}dE$$

and

$$I'(V) = AN_0\left[\frac{1}{kT}e^{V/kT}\int_V^\infty \sigma(E)\,e^{-E/kT}dE - \sigma(V)\right],$$

whence

$$\sigma(V) = \frac{I(V) - kTI'(V)}{AN_0kT}.$$

The quantity

$$N_0kT = \int_0^\infty N_0 e^{-U/kT}dU$$

is the total electron current. Determining the effective value of kT from the slope of the function $\log I_e = f(-V)$, finding I'(V) by graphical differentiation of I(V), we can ascertain the true dependence of cross section on electron energy.

The cross-section curves for a given molecule, obtained in different experiments, were averaged over the points. The mean-square error for each point is less than 15 to 20%.

1. SF_6, CCl_4 and CF_3I. If the width of the capture region is much smaller than the width of the electron energy distribution the ion-current curve should be similar to the distribution curve and the displacement of the ion current peak with respect to the distribution peak characterizes the energy at which capture takes place. In an earlier report[3] it was shown that these curves are, in fact, similar for SF_6 and CCl_4; hence the width of the capture region in these cases is several hundred

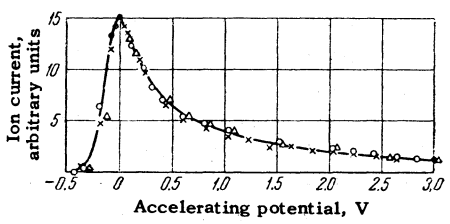

FIG. 1. Negative ion current in SF_6.

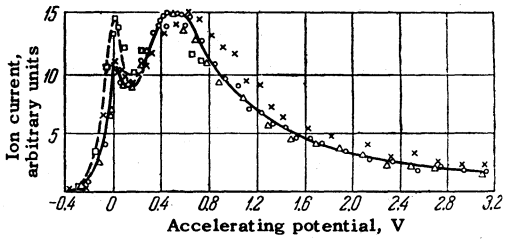

FIG. 2. Negative ion current in CCl_4.

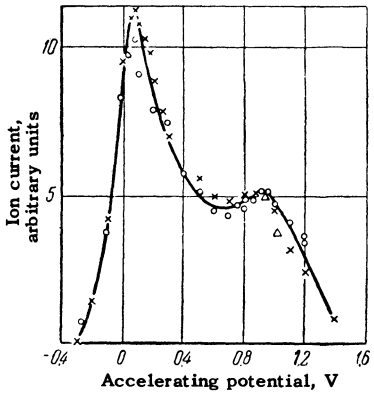

FIG. 3. Negative ion current in CF_3I.

electron volts. The displacements of the peaks are 0 ± 0.01 ev for SF_6 and 0.02 ± 0.01 ev for CCl_4. In CF_3I it is also found that the ion current curve is similar to the distribution curve and that the ion current peak is displaced with respect to the distribution maximum by 0.05 ± 0.01 ev (average of four measurements).

Figures 1 to 3 show the ion current as a function of accelerating potential for SF_6, CCl_4 and CF_3I. In each figure are shown the data of three different experiments. The ion current is given in arbitrary units and is adjusted to obtain coincidence of the peaks obtained in different experiments. The energy scale is given with respect to the position of the first ion-current peak.

It has been shown by mass-spectrometer studies[4,5] that in SF_6 the ions SF_6^-, SF_5^-, and F^- are formed in this energy region. According to the data reported in reference 4 the SF_6^- current is shifted with respect to the electron peak by 0.1 ev; the width of the region in which SF_5^- is formed is approximately 1 ev. The ratio of the maximum SF_6^- current to the maximum SF_5^- current is approximately 25. The F^- current is approximately 100 times smaller than the SF_5^- current.

Thus, the curve shown in Fig. 1 represents the total current for SF_6^-, SF_5^- and F^-. The current at the maximum is mainly the SF_6^- current. It is apparent from Fig. 1 that when the acceleration potential is greater than 1.5 volts the current does not change very much as the electron energy is varied. Since the F^- current is very small, it is reasonable to assume that the collector current in this region is due to scattered electrons. To compute the cross section the current of scattered electrons was taken equal to two units on the scale in Fig. 1.

Figure 2 shows the ion current curve for CCl_4. The data obtained in the different experiments are consistent, with the exception of a discrepancy in the region of the first peak. The discrepancy is explained by the fact that Curve 1 (dotted) was taken at zero collector potential. In this case the width of the electron energy distribution is considerably smaller than in the other experiments. The discrepancy in this region is not important as far as a determination of the cross sections is concerned since these cross sections are determined by measurements at zero collector potential.

A number of workers have observed the formation of negative ions in CCl_4.[6-10] The appearance potentials for these ions are as follows:

Ion	Appearance Potential, ev		Probability	
Cl^-	0.2 [8],	~0 [10]	$CCl_4 + e \rightarrow CCl_3 + Cl^-$	(1)
Cl_2^-	—	0.8	$CCl_4 + e \rightarrow CCl_2 + Cl_2^-$	(2)
CCl_3^-	—	1.4	$CCl_4 + e \rightarrow Cl + CCl_3^-$	(3)

According to the data of reference 10 the Cl_2^- peak is approximately 45 times smaller than the Cl^- peak while the CCl_3^- peak is approximately 450 times smaller than the Cl^- peak. For this reason the second maximum observed on the curve in the present work cannot be attributed to Cl_2^- or CCl_3^-. It is apparently explained by the process given in (1), with the transition to another potential curve of the intermediate ion CCl_4^-. The second maximum has also been observed in reference 9, in which a Lozier apparatus was used. The fact that this maximum has not been observed by other workers is explained by the large width of their energy distributions. Actually, it has been found[8] that the appearance potential for negative ions is 0.2 ev while the ion current peak is at 1.7 ev; whence it follows that the width of the energy distribution in these experiments was not smaller than 2 or 3 ev. It is natural that the first and second maxima would not be resolved under these conditions.

As is apparent from Fig. 2, the ion current becomes relatively insensitive to energy at electron energies greater than 2 ev. In computing the cross section it was assumed that the current due to scattered electrons was equal to 3 units on the scale in Fig. 2.

A curve showing the dependence of ion current on accelerating potential for CF_3I is shown in Fig. 3. The formation of negative ions in CF_3I has been studied earlier in reference 11 to 13. The following appearance potentials were found:

Ion	Appearance Potential, ev			Probability	
F^-	1.5 ± 0.2 [13];	3.6 ± 0.3 [12],	~0 [11]	$CF_3J + e \rightarrow CF_2J + F^-$	(4)
J^-	~0	~0	~0	$CF_3J + e \rightarrow CF_3 + J^-$	(5)

In this case the I^- current at 0 ev is 10 times larger than the F^- current. Thus, there is little

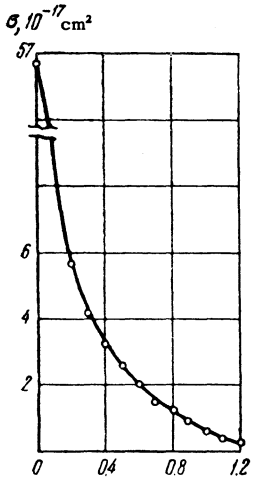

FIG. 4. Electron capture cross sections in the molecule SF_6.

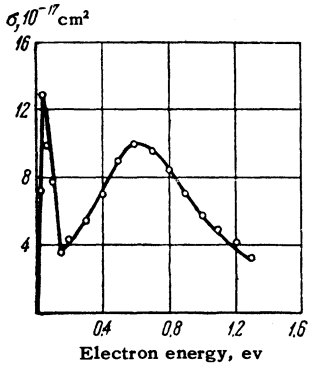

FIG. 5. Electron capture cross sections in the molecule CCl_4.

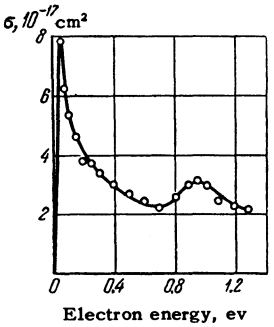

FIG. 6. Electron capture cross sections in the molecule CF_3I.

doubt that the narrow maximum at 0.05 ev is due to the process in (4). The origin of the second maximum is not clear. It arises either as a result of (4) with transition to another potential curve of CF_3I, or by virtue of the process in (5). The curve shown in Fig. 3 was taken at zero collector potentials since the current due to scattered electrons was negligibly small.

Figures 4 to 6 show the capture cross sections σ as functions of electron energy for SF_6, CCl_4 and CF_3I. In computing the cross section in the energy region 0 to 0.2 ev only the data obtained in experiments with zero collector potential were used.

2. CCl_2F_2. Figure 7 shows the ion current as a function of accelerating potential for CCl_2F_2. In this same figure the dashed curve denotes the electron energy distribution. The shape of the beginning of the ion current curve is similar to the distribution curve. This indicates that the cross section increases from zero to maximum in an energy region which is small compared with the distribution width. The curve has a flat maximum which is 0.12 volts wide. The beginning of the maximum is shifted with respect to the electron energy peak by 0.07 ± 0.01 volts (average of six measurements). There are no reliable data on the formation of negative ions in CCl_2F_2 so that the observed effects could not be interpreted.

A curve showing the capture cross section as a function of electron energy is given in Fig. 8.

3. BCl_3. A curve for the negative ion current in BCl_3 is shown in Fig. 9. The initial part of the curve is again similar to the electron curve (dashed). The curve has a flat maximum 0.2 volts wide. The beginning of the maximum is shifted with respect to the peak in the electron distribution by 0.23 ± 0.01 ev (average of six measurements). The dependence of capture cross section on electron energy is given in Fig. 10. The formation of Cl^- at electron energies close to zero has been observed by a mass-spectrometer measurement in BCl_3.[14] The authors, however, think it is possible that the Cl^- ions are formed because of HCl impurities. The present results indicate that the negative ions in BCl_3 are in fact a result of the reaction $BCl_3 + e \rightarrow BCl_2 + Cl^-$, since the maximum in the negative ion current in HCl oc-

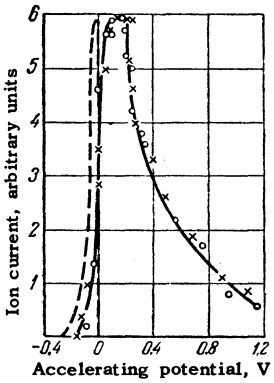

FIG. 7. Negative ion current in CCl_2F_2.

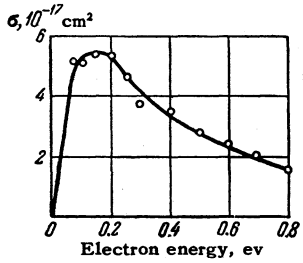

FIG. 8. Electron capture cross sections in the molecule CCl_2F_2.

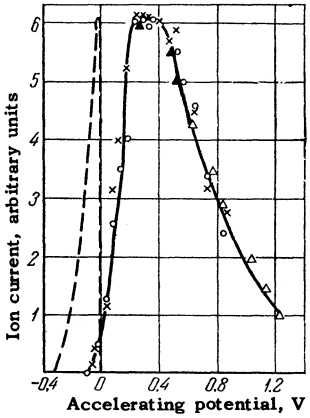

FIG. 9. Negative ion in BCl_3.

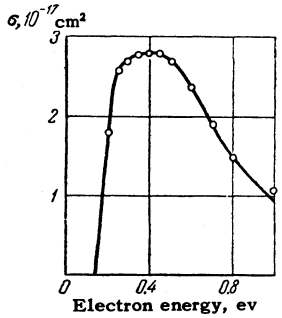

FIG. 10. Electron capture cross sections in the molecule BCl_3.

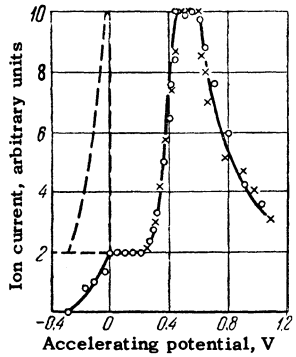

FIG. 11. Negative ion current in HCl.

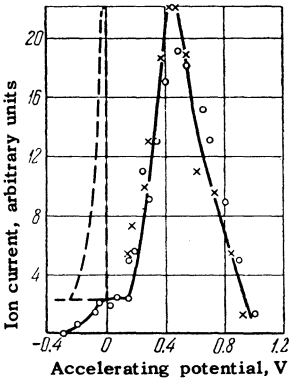

FIG. 12. Negative ion current in HBr.

curs at an electron energy of 0.05 ev and the HCl capture cross section is of an order of magnitude smaller than that observed for BCl_3.

4. HCl and HBr. The ion current curves for HCl and HBr are given in Figs. 11 and 12. In these cases scattering is important even at zero collector potentials since the initial part of the ion current curve (up to 0.25 volts for HCl and up to 0.15 volts for HBr) is determined by the scattered electrons. The curve showing the increase in ion current in these cases is similar to the electron energy distribution curves. The ion current curves have flat maxima. The shift of the beginning of the maximum with respect to the distribution peak for HCl is 0.46 ± 0.02 volts (average of six measurements); in HBr this shift is 0.43 ± 0.01 volts (average of four measurements). The width of the maximum in HCl is 0.15 volts; in HBr it is several hundredths of a volt.

The appearance potentials for Cl^- in HCl and Br^- in HBr in this energy region have been determined by mass-spectrometer methods. The following results were obtained:

Ion	Appearance Potential, ev	Probability
Br^-	0.6 ± 0.3 [10]	$HBr + e \rightarrow H + Br^-$
Cl^-	0.8 ± 0.3 [16]; 0.4 [10]; 0.66 ± 0.02 [15]	$HCl + e \rightarrow H + Cl^-$

The value 0.66 ± 0.02 ev was found by Fox for the shift in the Cl^- peak with respect to the SF_6^- peak in a mass-spectrometer investigation of the negative ions in HCl, using a nearly-monoenergetic electron beam. Since the SF_6^- peak occurs at zero electron energy, the shift in the Cl^- peak with respect to the SF_6^- peak should be the same as the shift in the Cl^- peak with respect to the electron peak. However, in the present case a flat maximum is observed; the maximum extends from 0.46 ± 0.02 ev to 0.62 ± 0.01 ev. The discrepancy may be explained by the difference in the shape of the energy distribution in the present experiments as compared with those in the Fox experiments. Since the distribution in the Fox experiments did not have a sharp cut-off, the ion current peak may be in the middle or at an extremity of the region in which the capture cross section is not strongly affected by energy. The width of the distribution in the Fox experiments (approximately 0.5 ev) was larger than the width of this region whereas in the present case approximately 60% of the electrons have energies within an interval of 0.1 ev and the total width of the distribution is 0.25 to 0.30 ev. The distribution has a sharp edge on the low energy side so that the beginning of the ion peak should coincide with the beginning of the region in which the cross section is not a strong function of energy.

Curves showing the dependence of capture cross section on electron energy are given in Figs. 13 and 14. The capture probability and the electron sticking coefficient for HCl have been measured earlier by diffusion methods.[17,18] An estimate of the capture cross section on the basis of the data reported in reference 17 shows that the cross section at the maximum is of the order of 10^{-18} cm^2; this result is in good agreement with the value obtained in the present work, 4×10^{-18} cm^2.

5. O_2 and H_2O. These measurements were

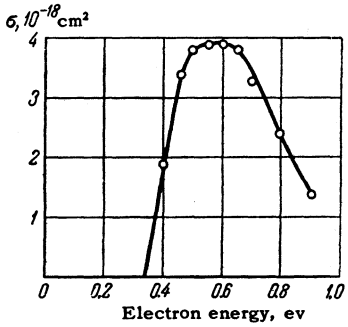

FIG. 13. Electron capture cross sections in the molecule HCl.

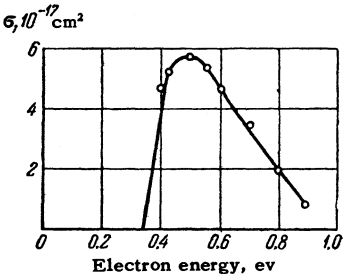

FIG. 14. Electron capture cross sections in the molecule HBr.

carried out in the electron energy ranges 0 to 8 ev for O_2 and 0 to 10 ev for H_2O. It has been shown by mass-spectrometer measurements that the following processes occur in this energy region:

Process	Appearance Potential, ev	
$O_2 + e \rightarrow O + O^-$	4.7 ± 0.1 [8,19,20]	(6)
$H_2O + e \rightarrow H^- + OH$	5.6 ± 0.5 [21,22]	(7)
$H^- + OH$	(maximum at 7.1 ev)	(8)
$O^- + 2H$	7.5 ± 0.3	

In the present case the appearance potentials are determined from the ion current curve. Under these conditions the electron energies are given by the accelerating potential. The zero of the energy scale is established by compensation of the contact potentials of the grids which define the equipotential region and is verified by the position of the peak in the electron energy distribution. It is found that the position of the peak in the distribution does not depart from $V = 0$ by more than 0.02 or 0.03 ev.

Although a nearly-monoenergetic electron beam is used, in determining the appearance potentials one must take account of the width of the electron energy distribution. This procedure is carried out as follows.[23] As has been indicated above, the dependence of ion current on accelerating potential is of the form

$$I(V) = \int_0^\infty A\sigma(E) N_0 e^{-U/kT}\, dU = N_0 \int_0^\infty p(E)\, e^{-U/kT} dU,$$

where $p(E)$ is the capture probability. Let the appearance potential be A. Then for $E < A$, $p(E) = 0$. We assume that when $E > A$,

$$p(E) = a(E - A)^n.$$

Considering the cases $n = 1$ and $n = 2$ we find for the first case:

$$d \ln I_i / dV = 1/kT \text{ for } V \leqslant A;$$
$$d \ln I_i / dV = 1/(kT + V - A) \text{ for } V > A.$$

In the second case:

$$d \ln I_i / dV = 1/kT \text{ for } V \leqslant A;$$
$$d \ln I_i / dV = 2(V - A + kT)/[k^2T^2 + (V - A + kT)^2] \text{ for } V > A.$$

Thus, assuming a linear or quadratic dependence of electron capture probability on energy, the function $\ln I_i = f(V)$ is a straight line with slope $1/kT$ up to the point $V = A$, at which the accelerating voltage is equal to the appearance potential. For $V > A$, $\ln I_i$ is some other curve. The appearance potential can be found by determining the point at which the transition from the straight line to the other curve takes place.

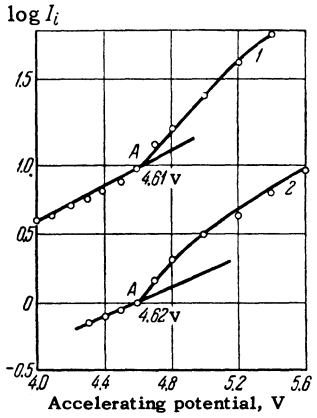

FIG. 15. The quantity $\ln I_i = f(v)$ as a function of accelerating potential for O_2. 1) total ion current 2) current of the monoenergetic component.

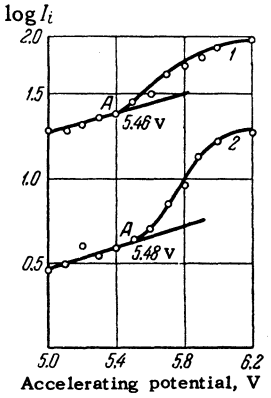

FIG. 16. The quantity $\ln I_i = f(v)$ as a function of accelerating potential for H_2O. 1) total ion current 2) current of the monoenergetic component.

Figures 15 and 16 show the dependence of the logarithms of ion current on accelerating potential. It is apparent from the figures that the initial part of the function $\ln I_i$ is actually a linear function of V. The appearance potential is determined from the transition point between the linear segment and the curvilinear segment (A on the figures). It was found that the appearance potential for O^- in O_2 is 4.63 ± 0.04 ev (average of fifteen measurements); the appearance potential for H^- in H_2O is 5.45 ± 0.09 ev (average of nine measurements). It should be noted that the uncertainty in the given energy scale appears in the spread of the appearance potentials.

The appearance potential for O^- is frequently used as a standard for calibrating energy scales in determining the appearance potentials for negative ions. However, the available data are not consistent. Thus, in the work reported by Lozier[24] it was found that $A(O^-)$ is 4.8 ev. McDowell and Warren,[25] taking the appearance potential of O^- in CO as 9.3 ev, found $A(O^-)$ to be 4.9 ± 0.1 ev. The most reliable value of $A(O^-)$ has been obtained by Marriott and Craggs[8] using a Lozier apparatus. Calibrating the energy scale by the appearance potential of the O_2^+ ion, 12.19 ev, these workers found that $A(O^-) = 4.7 \pm 0.1$ ev. The value found by us for the O^- appearance potential, 4.63 ± 0.04 ev, is in good agreement with the value 4.7 ± 0.1 ev, which was obtained with better accuracy. It should be emphasized that in the present case the appearance potential is determined on an absolute scale without reference to any standard.

In computing the capture cross section the cur-

rent due to scattered electrons was subtracted from the ion collector current; this electron current was taken equal to the collector current at at accelerating potential smaller than the appearance potential. In O_2 the scattered-electron current was 1 or 2%; in H_2O it was 5 to 10%. The presence of an electron energy distribution was taken into account only in the initial part of the curve. Since the width of the capture region is large compared with the width of the distribution in the region far from the appearance potential, taking account of the distribution will not affect the results to any great extent. It should be noted that in spite of the magnetic field all the H^- and O^- ions must strike the collector since, according to the data in the literature, the kinetic energy of these ions is greater than 1.5 ev.[21,24]

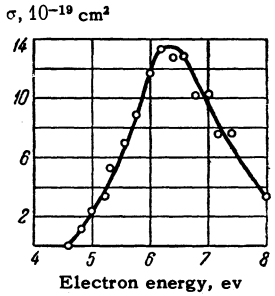

FIG. 17. Electron capture cross section in the molecule O_2.

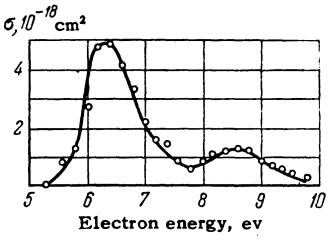

FIG. 18. Electron capture cross section in the molecule H_2O.

Curves showing the dependence of capture cross section on electron energy for O_2 and H_2O are given in Figs. 17 and 18. In O_2 the cross section peak occurs at an energy of 6.2 ev, $\sigma_{max} = (1.3 \pm 0.2) \times 10^{-18}$ cm^2 (average of seven measurements). In H_2O the first peak occurs at $\epsilon = 6.4$ ev, $\sigma_{max} = (4.8 \pm 1.5) \times 10^{-18}$ cm^2; the second peak occurs at $\epsilon = 8.6$ ev, $\sigma_{max} = (1.3 \pm 0.1) \times 10^{-18}$ cm^2 (average of eight measurements).

The second peak on the H_2O curve is apparently due to the formation of excited H_2O^-, which dissociates into H^- and OH. It should be noted that at electron energies greater than 7.5 ev the H^- current is somewhat high because of O^-, although, according to the data of reference 21, the maximum O^- current is approximately four times smaller than the H^- current.

The value of the capture cross section for O_2 at the peak has recently been determined by the single-collision method.[26] The measurements were carried out in a Lozier apparatus, using a magnetic field of approximately 200 oersteds. The capture cross section was determined from the ionization cross section for O_2 or Ar by a comparison of the positive and negative ion currents. Since no measures were taken to avoid the effects of space charge, the cross section determined in this way depends on electron current. Furthermore, a dependence of cross section on pressure and magnetic field was observed as a result of changes in scattering and changes in the electron path length with changes in p and H. To avoid these errors the curves showing the dependence of σ^- on I_e, p and H were extrapolated to the zero values. In making the calculations the values of σ^+ determined in refereces 27 and 28 were used.

The measurements show that the capture cross section at the peak is $(2.25 \pm 0.3) \times 10^{-18}$ cm^2 (average of four measurements). Taking account of the errors pointed out above and possible errors in the values of σ^+ it may be assumed that this value is in agreement with the value found in the present work $(1.3 \pm 0.2) \times 10^{-18}$ cm^2.

6. The table below lists the values of the electron capture cross sections at the peaks and the electron energies at which the peaks occur.

A tendency toward increased cross section with increased molecular complexity can be discerned. It is characteristic that in all the molecules containing halogens which have been investigated the capture cross section increases sharply in the region of the appearance potential. All the molecules which contain halogens have a capture region whose width is approximately several tenths of an electron volt at electron energies of the order of tenths of an

Molecule	Cross section at the first maximum, cm²	Electron energy at the first maximum, ev	Cross section at the second maximum, cm²	Electron energy at the second maximum, ev	Relative dielectric strength*
SF_6	$5.7 \cdot 10^{-16}$	0.00	—	~0.1 [4]	2.3—2.5 [29]
CCl_4	$1.3 \cdot 10^{-16}$	0.02	$1.0 \cdot 10^{-16}$	0.6	6.3 [29]
CF_3J	$7.8 \cdot 10^{-17}$	0.05	$3.2 \cdot 10^{-17}$	0.9	—
CCl_2F_2	$5.4 \cdot 10^{-17}$	0.15			2.4—2.5 [29]
BCl_3	$2.8 \cdot 10^{-17}$	0.4			—
HBr	$5.8 \cdot 10^{-17}$	0.5			2.2 [30]
HCl	$3.9 \cdot 10^{-18}$	0.6			1.5 [30]
H_2O	$4.8 \cdot 10^{-18}$	6.4	$1.3 \cdot 10^{-18}$	8.6	—
O_2	$1.3 \cdot 10^{-18}$	6.2			—

*With respect to $N_2 = 1$.

electron volt. Further, the more complicated molecules (SF_6, CCl_4 and CF_3I) have a capture region whose width is of the order of hundredths of an electron volt at electron energies of the same order of magnitude. O_2 and H_2O capture electrons with energies of several electron volts and the width of the capture region is also several electron volts.

The observed capture reactions can be explained in terms of rotational (hundredths of electron volts) or vibrational (tenths of electron volts) excitation of the molecule upon collision with the electron and subsequent capture of the electron. As has been shown theoretically[31,32] and experimentally,[33,34] in the molecules H_2 and N_2 the excitation cross sections for the vibrational and rotational levels increase sharply in the threshold energy region (hundredths of electron volts for rotational levels and tenths of electron volts for vibrational levels). The same dependence of capture cross section on electron energy near the appearance potential has been observed in the present case. Capture of this type can be interpreted by the intersection of the potential curve for the negative ion with the potential curve of the neutral ion at a point corresponding to an excited level. In O_2 and H_2O the potential curve for the negative ion lies considerably above the curve for the molecule so that this transition requires an energy of the order of several electron volts.

It is interesting to consider the SF_2^- ion. This ion is apparently an excited ion and the excitation energy, which exceeds the S-F binding energy, is distributed in the different vibrational and rotational degrees of freedom.[4]

A determination of the capture cross sections for slow electrons is of great interest in connection with the dielectric strength of gases. It may be assumed[29,35,36] that a higher dielectric strength is to be associated with a lower value of the Townsend coefficient α. Obviously the coefficient α is reduced with increasing electron capture.

The last column of the table lists values for relative dielectric strength. It is evident from the table that there is some correlation between the values of the capture cross section and the dielectric strength. Complete agreement is not to be expected since the measured cross sections (aside from SF_6) are cross sections for dissociative capture. At high pressures triple collisions are of greatest importance. In this case the capture probability can increase by virtue of stabilization of the molecular ion.

At low pressures, if the greater part of the unstable molecular ions decay with electron detachment, the capture probability with stabilization may increase many fold. On the other hand, if the molecular ions dissociate completely an increase in pressure will have essentially no effect on the capture probability. It is possible that this is the case in HCl and HBr. The cross section for dissociative capture in HBr is larger than the capture cross section in HCl and the dielectric strength in HBr is also greater than the dielectric strength of HCl. The increase in capture cross section, which is characteristic of increasing molecular complexity, may explain the increase in dielectric strength with increasing molecular weight of the gas which has been frequently observed.

I wish to thank V. L. Tal'roze for his interest in the work and valuable comments.

[1] N. S. Buchel'nikova, Приборы и техника эксперимента (Instruments and Measurement Engg.) **6**, (1958).

[2] Fox, Hickam, Grove, and Kjeldaas, Rev. Sci. Instr. **26**, 1101 (1955).

[3] N. S. Buchel'nikova, J. Exptl. Theoret. Phys. (U.S.S.R.) **34**, 519 (1958), Soviet Phys. JETP **7**, 358 (1958).

[4] W. Hickam and R. Fox, J. Chem. Phys. **25**, 642 (1956).

[5] A. J. Ahearn and N. Hanney, J. Chem. Phys. **21**, 119 (1953).

[6] R. Baker and J. Tate, Phys. Rev. **53**, 683 (1938).

[7] Craggs, McDowell, and Warren, Trans. Faraday Soc. **48**, 1093 (1952).

[8] J. Marriott and J. Craggs, Electr. Res. Assoc. Rep. L/T308, (1954).

[9] Marriott, Thurburn, and Craggs, Proc. Phys. Soc. (London) **B67**, 437 (1954).

[10] Reese, Dibeler, and Mohler, J. Res. NBS **57**, 367 (1956).

[11] J. Marriott, Electr. Res. Assoc. Rep. L/T301 (1953).

[12] Dibeler, Reese, and Mohler, J. Res. NBS **57**, 113 (1956).

[13] J. Marriott and J. Craggs, J. Electronics **1**, 405 (1956).

[14] J. Marriott and J. Craggs, J. Electronics **3**, 194 (1957).

[15] R. Fox, J. Chem. Phys. **26**, 1281 (1957).

[16] H. Gutbier and H. Neuert, Z. Naturforsch **9a**, 335 (1954).

[17] R. Healey and J. Read, The Behavior of Slow Electrons in Gases, Sydney 1941.

[18] N. Bradbury, Phys. Rev. **45**, 287 (1934).

[19] H. D. Hagstrum, J. Chem. Phys. **23**, 1178 (1955).

[20] R. Thorburn, Appl. Mass. Spectr. Conf. Rep., London Inst. Petroleum 1954.

[21] Mann, Hustrulid and Tate, Phys. Rev. **58**, 340 (1940).
[22] K. Laidler, J. Chem. Phys. **22**, 1740 (1954).
[23] R. E. Honig, J. Chem. Phys. **16**, 105 (1948).
[24] W. Lozier, Phys. Rev. **46**, 268 (1934).
[25] C. A. McDowell and J. Warren, Disc. Far. Soc. **10**, 53 (1951).
[26] Craggs, Thorburn, and Tozer, Proc. Roy. Soc. (London) **240A**, 473 (1957).
[27] J. T. Tate and P. T. Smith, Phys. Rev. **39**, 270 (1932).
[28] P. T. Smith, Phys. Rev. **36**, 1293 (1930).
[29] B. M. Gokhberg and E. I. Zandberg, Dokl. Akad. Nauk SSSR **53**, 515 (1946).
[30] C. Kowalenko, J. Phys. U.S.S.R. **3**, 455 (1940).
[31] Ta-You Wu, Phys. Rev. **71**, 111 (1947).
[32] E. Gerjuoy and S. Stein, Phys. Rev. **97**, 1671 (1955).
[33] J. Anderson and L. Goldstein, Phys. Rev. **102**, 388 (1956).
[34] R. Haas, Z. Physik **148**, 177 (1957).
[35] Warren, Hopwood, and Craggs, Proc. Phys. Soc. (London) **B63**, 180 (1950).
[36] Warren, Marriott, and Craggs, Nature **171**, 514 (1953).

Translated by H. Lashinsky
240